Nonuniform radiolabeling of VLDL apolipoprotein B: implications for the analysis of studies of the kinetics of the metabolism of lipoproteins containing apolipoprotein B

Rajasekhar Ramakrishnan, Yadon Arad, Steven Wong, and Henry N. Ginsberg[1]

Department of Medicine, College of Physicians and Surgeons, Columbia University, 630 West 168th Street, New York, NY 10032

Abstract Radiolabeling of whole lipoproteins or individual apolipoproteins has been an essential tool for the determination of the kinetics of apolipoprotein metabolism in vivo. Mathematical analysis of specific radioactivity (SA) or total radioactivity data has demonstrated the existence of significant complexity in the plasma decay curves of several apolipoproteins. Results obtained during development of methods to study the metabolism of apolipoprotein B (apoB) in very low density lipoprotein (VLDL) subclasses isolated according to flotation (S_f) rates from whole radiolabeled (d < 1.006 g/ml) VLDL suggested nonuniform radiolabeling of apoB in the three S_f subclasses being studied. We therefore determined apoB SA in VLDL S_f subclasses in ten hypertriglyceridemic and five normal subjects. After radioiodination of apoB in whole VLDL, different apoB SA were found in S_f 400–100, S_f 100–60, and S_f 60–20. The pattern of labeling was quite variable among subjects. On average, apoB SA in the VLDL tracer was greatest in S_f 400–100, and least in S_f 60–20. Nonuniform labeling could also be demonstrated in five studies in which samples were obtained 3 min after intravenous injection of the tracer into subjects with a wide range of plasma triglycerides. Nonuniform labeling of apoB in whole VLDL was also demonstrated in two of the subjects by isolating subclasses of their VLDL that did and did not bind to an anti-apolipoprotein E immunoaffinity column. These results indicate that the usual assumption of homogeneous labeling of apoB may be erroneous. We have derived a simple mathematical formula to study the consequences of this assumption in estimating kinetic parameters. It is shown that an erroneous assumption of homogeneous tracer labeling may significantly underestimate or overestimate the true production rate, even in a simple two-pool model. Identification of labeling characteristics and incorporation of this information into the mathematical analysis of the plasma radioactivity data can improve the accuracy of the analysis as well as the sensitivity of compartmental models generated by such data. —**Ramakrishnan, R., Y. Arad, S. Wong, and H. N. Ginsberg.** Nonuniform radiolabeling of VLDL apolipoprotein B: implications for the analysis of studies of the kinetics of the metabolism of lipoproteins containing apolipoprotein B. *J. Lipid Res.* 1990. **31:** 1031–1042.

Supplementary key words lipoproteins • kinetic analysis • compartmental models

Our ability to study the kinetics of lipoprotein metabolism in vivo has added significantly to our understanding of the regulation of plasma lipid levels in normal and dyslipidemic subjects. Mathematical analysis of either plasma total or specific radioactivity (SA) of particular apolipoproteins after radiolabeling whole lipoproteins has provided the basis for quantitating rates of production and catabolism of these apolipoproteins, for instance, very low density (VLDL), intermediate density (IDL), and low density lipoprotein (LDL) apolipoprotein B (apoB). These data, in turn, have demonstrated the in vivo consequences of mutations in the LDL receptor (1–3), the abnormalities present in VLDL production in individuals with various forms of hypertriglyceridemia (3–9), and the effects of mutations in apolipoprotein E (10–12) and apolipoprotein C-III (13) on VLDL and LDL apoB turnover in plasma. Direct study of the kinetics of metabolism of these latter apolipoproteins, as well as of apolipoprotein A-I and apolipoprotein A-II, has also provided invaluable information concerning the pathophysiology of various dyslipidemias.

It has been evident from the first studies of this type that significant complexity characterizes the plasma decay kinetics of the various tracers that have been used (14, 15). The turnover of apoB in VLDL is known to be more complex than that of a single pool since the apoB SA in whole VLDL has been observed to be curvilinear on a semilogarithmic plot, that is, a multiexponential curve rather

Abbreviations: SA, specific activity; VLDL, very low density lipoproteins; LDL, low density lipoproteins; IDL, intermediate density lipoproteins; TMU, 1,1',3,3'-tetramethylurea; FCR, fractional catabolic rate.

[1]To whom reprint requests should be addressed.

than a monoexponential curve. This has necessitated the development of various compartmental models to describe the plasma turnover of apoB (16), ranging from a simple two-pool model (17, 18) to models with cascades of varying lengths and remnant pools (19–23). These models differ in the number of pools, pool masses, pool turnover rates, interconnectivity among the pools, sites of de novo secretion, sites of conversion of VLDL to IDL and LDL, and sites of direct removal of apoB from plasma. One assumption, however, has been common to all the models, that is that all apoB VLDL pools are initially labeled equally by the injected bolus. In other words, the initial specific activities were assumed to be the same in all the pools within VLDL. This assumption was entirely reasonable as it allowed excellent fits of the observed SA data, and because there were no data addressing the issue of nonuniform labeling. In recent studies in our laboratory, in which radiolabeled whole ($d < 1.006$ g/ml) VLDL has been used as a tracer for the transport of apoB through VLDL subclasses isolated by flotation rates, we have observed differential, nonuniform labeling of apoB within these subclasses. These data, and a discussion of the implications for the mathematical analysis of kinetic data, are presented in this report.

METHODS

Subjects

Five normal subjects were recruited from the staff of the College of Physicians and Surgeons, and ten hypertriglyceridemic subjects from the lipid clinic of the Specialized Center of Research in Arteriosclerosis at the Columbia-Presbyterian Medical Center. Subjects who were undergoing studies of the in vivo turnover of VLDL apoB were admitted to the General Clinical Research Center at the Medical Center. The protocol for these turnover studies has been described in detail elsewhere (18). Subjects whose blood was used only for in vitro studies of apoB radiolabeling had samples obtained in our laboratory. These studies were approved by our Institutional Review Board and all subjects gave informed consent prior to participating.

Lipoprotein isolation

All blood samples were obtained after 12–14 h overnight fast. Blood was collected into sterile tubes containing EDTA (1.0 mg/ml) and the plasma was isolated by centrifugation at 2000 rpm, 4°C for 20 min. Whole ($d < 1.006$ g/ml) VLDL was isolated by sequential ultracentrifugations in SW 28 and SW 40 rotors at 23,000 and 39,000 rpm, respectively, at 10°C for 20 h (18). Whole VLDL isolated in this manner was used for iodination using iodine monochloride by the method of McFarlane (24) as modified by Bilheimer, Eisenberg, and Levy (14). Lipid labeling was always less than 15% and less than one atom of ^{125}I was incorporated per particle. Unreacted, free ^{125}I was removed by extensive dialysis in sterile 0.15 M NaCl (pH 7.4, 0.1 mg/ml EDTA). In general, the specific radioactivity of the iodinated preparation ranged from 75 to 200 μCi/mg of apoprotein. In some studies, we varied the quantity of ^{125}I used in order to obtain high and low specific activities of separate aliquots of the same VLDL preparation.

When the iodinated VLDL was used for an in vivo apoB turnover study, the whole VLDL preparation was mixed with human serum albumin, passed through a 0.45-μm Millipore filter, and injected intravenously (50 μCi) into the donor subject. Timed blood samples were obtained after injection and VLDL was isolated from each sample by ultracentrifugation of 3 ml plasma in a 50.3 Ti rotor at 39,000 rpm at 10°C for 20 h (18). Each VLDL sample was subjected to a second ultracentrifugation in an SW 40 rotor according to the method of Lindgren, Jensen, and Hatch (25) in order to isolate S_f 400–100, S_f 100–60, and S_f 60–20.

The labeled preparations were characterized in three ways. First, in ten subjects, a trace amount of each individual's radiolabeled whole VLDL was added to an aliquot of their own, unlabeled VLDL preparation in order to "spike" the unlabeled preparation. This sample was incubated at 37°C for 30 min, subjected directly to the gradient devised by Lindgren et al. (25), and the three VLDL S_f subclasses were isolated. Second, in the other five subjects, a trace quantity of radiolabeled whole VLDL was added to a blood sample obtained just prior to injection of the tracer, and this sample was then processed exactly as the 18 blood samples obtained after the injection (described above). Finally, in two subjects, in an attempt to further define the characteristics of the populations of VLDL that were labeled nonuniformly, we also used immunoaffinity chromatography with an anti-apoE Sepharose column to isolate apoE-deficient and apoE-enriched VLDL subpopulations from whole VLDL (26). Whole, radiolabeled VLDL, prepared as described above, was passed through an anti-apoE Sepharose column and both the void and bound fractions were collected. The bound VLDL fraction was eluted from the column with 0.2 M glycine, pH 2.5. We have previously determined that this elution protocol allows for the isolation of intact lipoprotein particles (26). A separate aliquot of each subject's radiolabeled whole VLDL was used to isolate the three VLDL S_f subclasses by density gradient ultracentrifugation.

Determination of apoB specific radioactivity

The SA of apoB in whole VLDL, in the VLDL S_f subclasses, and in apoE-deficient and apoE-enriched VLDL subpopulations was determined using 1,1',3,3'-tetramethylurea (TMU) as we originally described (27). This method

includes sequential delipidations with acetone and isopropanol prior to two further delipidations and selective precipitation of apoB with TMU. ApoB SA was determined in triplicate in four hypertriglyceridemic subjects but only in single samples (because of low apoB levels) in the rest of the subjects. In some studies, the final apoB pellet was subjected to an additional lipid extraction with chloroform. The method of determining apoB SA with isopropanol alone, reported by Egusa et al. (28), was also compared to the TMU method in studies of two separate subjects.

Although the original validation of the TMU method for determination of apoB SA included studies demonstrating that the final apoB pellets from VLDL, IDL, and LDL were not contaminated by other apolipoproteins (27), we addressed this issue in the VLDL S_f subclasses isolated in the present studies. Radiolabeled whole VLDL from an additional subject was ultracentrifuged through a density gradient (25) and S_f 400–100, S_f 100–60, and S_f 60–20 fractions were isolated. ApoB SA was determined using the TMU method (27) in aliquots of the original whole, radiolabeled VLDL and of each VLDL S_f subclass. Parallel aliquots were subjected to the same TMU protocol (27) but the apoB pellets were resolubilized by incubation under nitrogen in 100 mM sodium-dodecyl sulfate (SDS) for 48 h at 37°C. Because it is very difficult to resolubilize delipidated apoB that has been precipitated in TMU, a relatively large volume of SDS (50 μl) was required to achieve solubilization. This necessitated that multiple 5-μl samples (the maximal volume that could be used at one time) be sequentially loaded (every 10–15 min) onto a 2–16% polyacrylamide vertical slab gel. The gel was run overnight at 15 mA, at which time each of the prestained molecular weight markers, which were run separately in the first and last lanes and which were also loaded repeatedly, had all merged in the gradient gel. The gel was cut vertically into lanes and then each lane was cut into 2- to 3-mm horizontal strips. Radioactivity in each strip was determined in a gamma counter.

RESULTS

Two types of studies were conducted to insure that the TMU method could accurately determine apoB SA in VLDL S_f subclasses. First, we compared the apoB SA in each S_f subclass obtained using the TMU method (27) with the apoB SA determined using the method of Egusa et al. (28). In the first experiment, the apoB SA values in S_f 400–100, S_f 100–60, and S_f 60–20 fractions were 403, 279, and 289 cpm/μg, respectively, by TMU, and 523, 332, and 353 cpm/μg, respectively, by the method of Egusa et al. In a second experiment, the respective apoB SA values were 1610, 779, and 644 cpm/μg, respectively, by the TMU method, and 1615, 840, and 657 cpm/μg, respectively, by the method of Egusa et al.

Second, in order to exclude differential contamination of any VLDL S_f subclass apoB pellet with nonapoB apolipoproteins, SDS gel electrophoresis was performed with pellets from whole VLDL and each S_f subclass. The results (**Fig. 1**) demonstrate only a single region of radioactivity near the top of the 2–16% gel for whole VLDL and for each S_f subfraction. The fact that this region of radioactivity began at the top of the gel is consistent with either incomplete migration of some of the multiple aliquots of resolubilized TMU precipitate that we loaded onto the gel (see Methods), or some aggregation of resolubilized apoB. It is clear that there were no peaks of radioactivity in any other region of the gel. In addition, an identical peak near the top of the gel was obtained with radiolabeled LDL that had been subjected to the same protocol (data not shown). There were no significant differences in the patterns of radioactivity across the rest of the gel among the four samples. The pattern of low level radioactivity across the length of the gel present when VLDL was run was also present when LDL was run. The apoB SA values for VLDL S_f 400–100, S_f 100–60, and S_f 60–20 in this experiment were 61,056, 53,392, and 65,380 cpm/μg, respectively. The whole VLDL apoB SA was 56,958 cpm/μg. These results exclude significant contamination of the TMU pellets by apolipoproteins other than apoB as the basis of differences in the apoB SA of the S_f subclasses.

Table 1 presents the plasma lipids and apoB SA for seven subjects with elevated levels of plasma VLDL triglyceride (#1–7) and three normolipidemic individuals

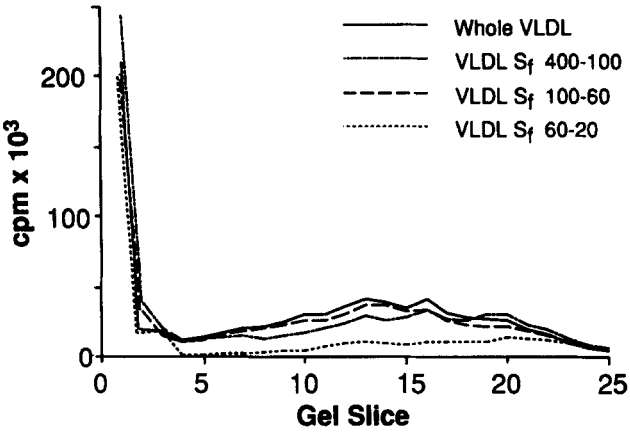

Fig. 1. Distribution of radioactivity in a 2–16% polyacrylamide gel. Aliquots of whole VLDL, S_f 400–100, S_f 100–60, and S_f 60–20 were subjected to the TMU method, the resulting apoB pellets were resolubilized, and the solubilized material was electrophoresed. The gels were cut into lanes, each lane was divided into 2- to 3-mm slices, and the radioactivity was determined in a gamma counter. There was a single peak of radioactivity for each sample in the first two slices and there were no significant differences in the remaining slices among the samples.

TABLE 1. Distribution of apoB SA in VLDL subfractions[a]

No.	TG[b]	S_f 400–100	S_f 100–60 / S_f 400–100	S_f 60–20 / S_f 400–100
	mg/dl	*cpm/μg*		
1	250	491 ± 18[c]	0.43 ± 0.09	0.58 ± 0.01
	(chloroform)[d]	484 ± 50	0.40 ± 0.07	0.55 ± 0.002
2	280	1878 ± 47	0.59 ± 0.11	0.41 ± 0.07
	(chloroform)[d]	1604 ± 26	0.50 ± 0.11	0.36 ± 0.05
3	240	1619 ± 57	0.80 ± 0.05	0.46 ± 0.08
4[e]	210	25.9 ± 0.9	0.65 ± 0.06	0.51 ± 0.08
		100.8 ± 7.3	0.56 ± 0.08	0.54 ± 0.003
5[e]	450	6446	0.77	1.05
		147862	0.83	1.29
6	300	937	1.27	0.82
7	380	910	1.21	0.73
8	40	3890	0.32	0.36
9	80	2316	0.63	0.81
10	50	2165	0.61	0.87
Mean (± SD) of subject means			0.73 ± 0.31	0.66 ± 0.23

[a]Absolute apoB SA is presented for S_f 400–100. ApoB SA in S_f 100–60 and S_f 60–20 have been divided by the apoB SA in S_f 400–100.
[b]TG, plasma triglyceride level.
[c]Plus-minus values are standard deviations of triplicates.
[d]Subjects 1 and 2 had apoB SA determined before and after an additional delipidation of the apoB pellet by chloroform (see Methods).
[e]Subjects 4 and 5 had their whole VLDL samples labeled to two different specific activities prior to isolation of VLDL S_f fractions. The values for both sets of S_f fractions are given.

(#8–10); the samples were characterized after in vitro incubations. In each of these studies whole VLDL was initially isolated by sequential ultracentrifugations in SW27 and SW40 rotors, one aliquot of the VLDL was radiolabeled, and an aliquot of the unlabeled VLDL was spiked with a trace amount of labeled VLDL. Since the absolute values of SA in different subjects cannot be compared meaningfully, the SA in the two denser subfractions are presented in terms of the SA in S_f 400–100 for each individual. The ratios for apoB SA in S_f 100–60 and S_f 60–20 should be close to 1.0 if labeling of different subfractions is uniform. In seven out of the ten subjects, S_f 400–100 had a significantly greater apoB SA than the two denser subclasses. The apoB SAs in S_f 100–60 and S_f 60–20 were, on average, 73% and 66%, respectively, of that in S_f 400–100. In any individual, the pattern could be quite different; subjects 6 and 8 show two extremes. In four subjects, the analyses were done in triplicate. The coefficients of variation of the replicates were less than 11%, strengthening the findings that labeling of different subfractions is nonuniform and that the nonuniformity itself is variable from one individual to another.

An additional lipid extraction of the apoB pellet with chloroform in the studies of subjects 1 and 2 did not alter the results significantly. In subjects 4 and 5, we spiked two aliquots of their VLDL to obtain higher and lower SA levels. As expected, the absolute levels of apoB SA differed in the two samples, but the SA ratios of S_f 100–60:S_f 400–100 and of S_f 60–20:S_f 400–100 were similar in the two samples, showing that the patterns of differential labeling were unaffected by the quantity of labeled material added to their unlabeled VLDL.

The differential labeling of apoB in VLDL S_f subclasses could also be demonstrated during in vivo turnover studies of this apolipoprotein. Five subjects (#11–15) with a wide range of plasma triglyceride concentrations received injections of autologous, radiolabeled VLDL. An aliquot of tracer was used to spike a plasma sample obtained just prior to injection, and apoB SA was determined in this sample (injected material) as well as in the plasma sample obtained 3 min after injection. **Table 2** presents the results from these five subjects. In each sample, apoB SA was determined in whole VLDL as well as in the three subfractions. Subfraction SA values are reported in terms of whole VLDL SA. These ratios for the three subfractions should be close to 1.0 if labeling is uniform. Observed values show considerable nonuniformity. In subject 11, S_f 400–100 SA was only half that of whole VLDL while S_f 60–20 SA was about 1.4 times that of whole VLDL. Subject 12 showed the reverse: S_f 400–100 SA was about 1.5 times that of whole VLDL while S_f 60–20 SA was half that of whole VLDL. The 0-minute sample was spiked in vitro while the 3-min sample was subsequent to in vivo spiking with the administered tracer. With the exception of subject 13, there was fair agreement in the ratios of subfraction SA to whole SA between the spiked sample and the 3-min sample. This consistency lends support to the finding of nonuniform labeling. The proportion of labeled to unlabeled VLDL apoB in the spiked sample is different from the in vivo 3-min sample; therefore, whole VLDL SA are not comparable between the two. As in the subjects reported in Table 1, S_f 60–20 and S_f 100–60 were generally labeled to a lower SA than was S_f 400–100.

In the same five subjects, we estimated the mean apoB SA of the three S_f subclasses from the distribution of apoB mass among the subclasses, and calculated its ratio to the actually observed SA in whole VLDL; this is given in the final column of Table 2. Values close to 1.0 indicate good agreement between observed apoB SA for the whole VLDL preparation and the value calculated from the specific activities in the three subfractions. As noted above, only subject 13 (at 0 time) had a ratio of calculated to observed VLDL SA that was clearly less than 1.0.

VLDL apoB SA decay curves from two studies (subjects 12 and 13), in whom radiolabeled whole VLDL was injected, are depicted in **Fig. 2.** The apoB SA levels in S_f 400–100, S_f 100–60, and S_f 60–20 in samples obtained during the first 60 min after injection of radiolabeled whole VLDL are presented. The 3-min points for each subject correspond to the 3-min entries in Table 2. It can

TABLE 2. Comparison of apoB SA in VLDL S_f fractions isolated from injectate and from 3-min samples[a]

No.	TG[b]	Time[c]	Whole	S_f 400–100 / Whole	S_f 100–60 / Whole	S_f 60–20 / Whole	$Whole_{calc}$ / $Whole_{obs}$
	mg/dl		*cpm/μg*				
11	190	0	8.4	0.50	0.74	1.43	1.10
		3	16.2	0.49	0.46	1.25	1.20
12	480	0	100.0	1.50	1.01	0.45	0.90
		3	19.3	1.58	1.03	0.56	0.97
13	50	0	465.0	0.77	0.20	0.40	0.41
		3	107.5	1.42	1.15	0.75	0.88
14	520	0	26.4	0.83	0.81	0.53	0.70
		3	9.6	0.73	0.60	0.71	0.68
15	210	0	17.1	0.98	1.10	0.54	0.78
		3	8.9	0.61	1.04	0.57	0.72

[a]Absolute apoB SA is presented for whole VLDL ($d < 1.006$ g/ml). ApoB SA for S_f fractions are expressed in terms of whole VLDL apoB SA. The final column presents the ratio of whole apoB SA calculated from the SA values in each S_f subfraction and the determined apoB SA in whole VLDL.

[b]TG, plasma triglycerides.

[c]Time samples analyzed were 0: plasma obtained prior to injection of tracer into subject and then spiked with an aliquot of injected tracer; 3: plasma obtained 3 min after injection of tracer into subject.

be seen that the differences observed at 3 min persist with time, offering further evidence that nonuniformity of labeling is real and persists in vivo. After a few minutes, as the SA in S_f 400–100 drops due to dilution with newly secreted, unlabeled particles, the SA curves intersect. The rise in S_f 100–60 SA and the flat levels of S_f 60–20 SA are due to entry of tracer from more buoyant subfractions. If there were no tracer entry from more buoyant subfractions, the SA in S_f 100–60 and S_f 60–20 would drop rather than rise or remain flat.

While apoB SA did decline more rapidly in S_f 400–100 than in the other two subfractions, there was not much change in the first 10 min. Since we have three samples from each subject in the first 10 min, it is possible to look for consistency with sequential plasma samples in the nonuniformity of labeling. **Table 3** shows the subfraction SA data at 3, 6, and 10 min for subjects 11–15. It can be seen that while each subject had a different pattern of nonuniformity (in subject 11, the highest label was in S_f 60–20, while in subject 12, the highest label was in S_f

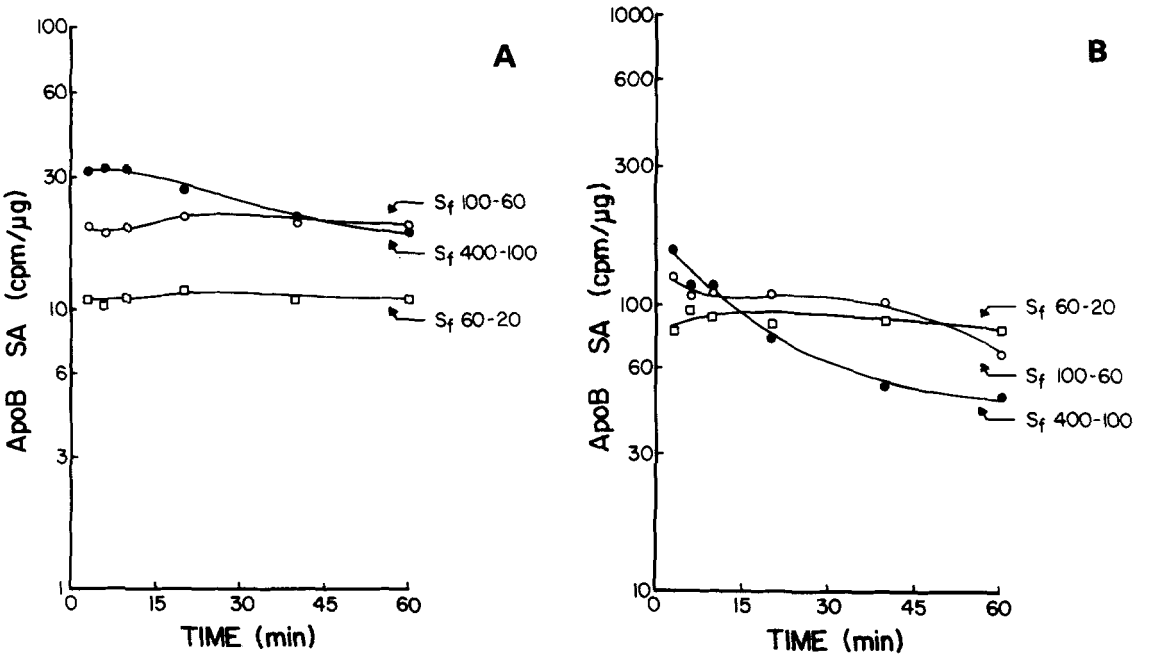

Fig. 2. ApoB SA in VLDL subfractions for the first 60 min after a bolus injection of radiolabeled whole VLDL. Lines are drawn freehand to provide visual continuity; A, subject 12; B, subject 13.

TABLE 3. Sequential apoB SA in five subjects

Subject	Time[a]	S_f 400–100	S_f 100–60	S_f 60–20
	min		*cpm/μg*	
11	3	7.9	7.5	20.2
	6	5.6	7.9	29.0
	10	4.1	7.9	27.0
12	3	30.5	19.8	10.9
	6	31.7	18.6	10.2
	10	31.1	19.6	10.9
13	3	152.9	123.7	80.4
	6	116.2	107.9	95.5
	10	119.8	107.8	89.5
14	3	7.0	5.8	6.8
	6	5.3	7.6	5.7
	10	7.3	8.3	7.6
15	3	5.4	9.3	5.1
	6	5.6	6.1	3.8
	10	4.8	3.1	3.1

[a]Time is of plasma sample.

400–100, etc.), the pattern in any one subject was consistent across the first three samples. The data in Table 3 were analyzed by a three-way analysis of variance (fixed-random-random corresponding to the subfractions, subjects, and time replicates). It was found that the interaction between subfraction and subject was highly significant ($F_{8,16} = 11.03$, $P < 0.00004$). This means, as is also apparent from a perusal of Table 3, that in each subject, the subfraction SA values are different from one another and that this difference varies from subject to subject.

To further define the physical-chemical characteristics of the differentially labeled subpopulations of VLDL, we utilized an entirely different method of isolating VLDL subclasses, namely immunoaffinity chromatography. **Table 4** presents the apoB SA in subjects 6 and 7, determined in whole VLDL, apoE-deficient VLDL (defined by the lack of binding to an anti-apoE immunoaffinity column), and apoE-enriched VLDL (defined by the ability to bind to that column). The latter two are expressed in terms of whole VLDL SA. The apoE content of fractions isolated in this manner, as determined by radioimmunoassay, was 1–3% of the total protein content in the apoE-deficient fraction, and 20–30% of the total protein content in the apoE-enriched fraction (26). In both subjects, the apoB SA in apoE-deficient VLDL was greater than that in the apoE-enriched fraction and was similar to the apoB SA in more buoyant VLDL (S_f 400–100 and S_f 100–60).

An unexpected finding was that all the S_f fraction: Whole SA ratios were greater than 1.0 in subjects 6 and 7. Although apoB masses were not determined in the three S_f fractions in these two experiments, our data in other studies (subjects 11–15) indicate that the large majority of apoB would have been in S_f 60–20. Hence, the "$Whole_{calc}$:$WholeS_{obs}$" VLDL SA (as in Table 2) would be close to that of S_f 60–20: Whole and not out of the range, therefore, of the values presented in Table 2. In any event, this discrepancy does not affect the comparison of the apoE-deficient and apoE-enriched fractions or their similarities to subfraction SAs.

DISCUSSION

Our results clearly indicate that radiolabeling of whole VLDL, isolated by standard ultracentrifugal methods, does not uniformly label subclasses of the VLDL defined either by flotation rate or by apolipoprotein composition. The basis for this lack of uniform labeling is unclear. The finding that in many cases the highest apoB SA was in S_f 400–100 suggests that a particular conformation of apoB in the more triglyceride-rich S_f fraction was associated with more efficient radiolabeling. Higher apoB SA values in apoE-deficient VLDL compared to apoE-enriched VLDL support this hypothesis as apoE-deficient VLDL are more triglyceride-enriched (29). The pattern of apoB SA in the different S_f fractions was not consistent, however. The relationship between our findings and previously published data (30) indicating changes in immunoreactivity of apoB across the VLDL S_f 400–100 range remains to be determined.

Regardless of the underlying mechanisms, however, these data raise questions about the accuracy of kinetic parameters estimated from past studies that analyzed only whole VLDL SA data with multicompartmental models. While there was no reason previously to assume nonuniform labeling, these new results make it necessary to study the possible consequences of erroneously assuming uniform labeling.

One approach would be to take data previously fitted with a model that assumed uniform labeling, reanalyze

TABLE 4. ApoB SA in apoE-deficient and apoE-rich VLDL fractions

Fraction	Subject 6	Subject 7
Whole VLDL	726.0	618.0 ± 25
ApoE-deficient:whole	1.26	1.86 ± 0.05
ApoE-rich:whole	0.95	0.65 ± 0.04
S_f 400–100:whole	1.29	1.47
S_f 100–60:whole	1.64	1.78
S_f 60–20:whole	1.06	1.07

In each study, whole VLDL was isolated and divided into three aliquots. One aliquot was used for apoB SA determination directly, one aliquot was subjected to density gradient ultracentrifugation to isolate three S_f fractions prior to apoB SA measurement, and one aliquot was passed through an anti-apoE IgG Sepharose column to isolate apoE-rich and apoE-deficient fractions prior to determination of apoB SA (cpm/μg). The results for subject 7 are means (± SD) of triplicates.

the data with a model that allows different initial apoB SA values in different VLDL pools, and compare the estimated kinetic parameters. A more general approach, taken here, is to derive mathematical formulas for the kinetic parameters estimated under the uniform labeling assumption in terms of the kinetic parameters of a model without uniform initial labeling. This latter approach has certain advantages in that the results are independent of measurement accuracy and times of observation, and that the comparison is with mathematical formulas rather than with particular SA so that the results can be generalized.

Since the kinetic parameter of greatest interest to investigators is the rate of production of VLDL apoB, the analysis presented here will be confined to a comparison of the production rate (R_{v0}) obtained in two ways: using a model that assumes uniform labeling or using a model that allows nonuniform labeling. The FCR of the tracee can be obtained by dividing R_{v0} by the measured mass of VLDL apoB.

Before considering a general model, it may be helpful to look at the simplest possible model. The initial rate of decline of the VLDL apoB activity curve equals the rate at which activity is leaving the VLDL range, which, in turn, for a single-pool model, equals the mass flux out of VLDL (i.e., apoB production or absolute catabolic rate) multiplied by the initial specific activity in VLDL. From this, we find

$$R_{v0} = \frac{\text{Initial Activity Slope}}{\text{Initial Specific Activity}}. \qquad \textit{Eq. 1)}$$

While this result is quite obvious for a single-pool model, we will derive a similar result below for a model with many pools and show how the denominator is different for a model with nonuniform labeling.

Consider **Fig. 3**, which shows a general n-pool model for the turnover of VLDL apoB. It is assumed that all n pools are circulating, intravascular pools. Let M_v equal the mass of apoB in VLDL; let m_i be the mass fraction of pool i (the mass of apoB in pool i is, therefore, m_iM_v); let the initial SA in pool i be u_i; and let R_{0i} be the flux out of VLDL from pool i (this flux includes conversion to IDL and/or LDL as well as direct removal from plasma; it does not include conversion to another VLDL pool). Using these defined terms, the initial rate of disappearance of activity in VLDL apoB is obtained by adding up the rates of disappearance out of the VLDL range from each pool within VLDL:

$$\text{Initial Activity Slope} = R_{01}u_1 + \ldots + R_{0n}u_n = \sum_{i=1}^{n} R_{0i}u_i. \qquad \textit{Eq. 2)}$$

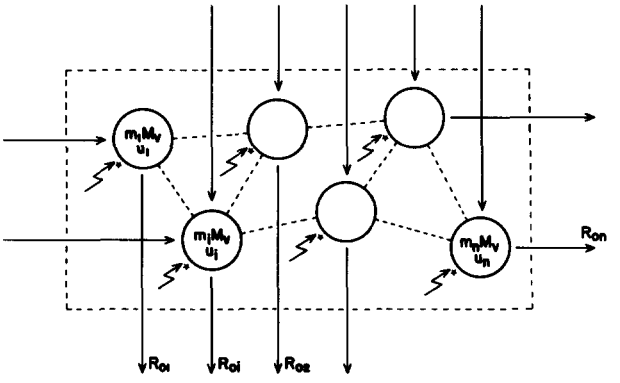

Fig. 3. A general n-pool model for the turnover of VLDL apoB. M_v is the total mass of apoB in VLDL; m_i is the mass fraction in the i-th pool; u_i is the initial SA in the i-th pool; R_{0i} is the apoB flux out of the i-th pool, converted to IDL and/or LDL or removed from plasma. The dashed lines among the pools indicate possible fluxes (in any direction). The dashed box surrounds pools that are intravascular and are included in the measurement of whole VLDL SA. In this case, all VLDL pools are circulating and intravascular, by assumption.

(The form $\sum_{i=1}^{n}$ is used as short-hand for summing up what follows ($R_{0i}u_i$ here) with i assuming all integer values from 1 to n. It is read as *sum from i equals 1 to n.*)

In terms of SA data (obtained by dividing both sides of the equation by M_v),

$$\text{Initial SA slope} = \sum_{i=1}^{n} R_{0i}u_i/M_v. \qquad \textit{Eq. 3)}$$

If the assumption of uniform labeling is made, the u_i values are all equal to one another as well as to u_v, the initial SA in whole VLDL apoB, and the expression in equation 2 becomes

$$\text{Initial Activity Slope} = \sum_{i=1}^{n} R_{0i}u_i = u_v \sum_{i=1}^{n} R_{0i} = u_vR_{v0} \qquad \textit{Eq. 4)}$$

Thus, if initial specific activities in all pools are equal, the production rate is obtained as

$$R_{v0} = \frac{\text{Initial Activity Slope}}{\text{Initial Specific Activity}}. \qquad \textit{Eq. 5)}$$

(It may be noted that equation 5 is identical to equation 1, though the result here is for a multicompartmental model.)

If SA data are used instead of total activity data, both sides of the equation can be divided by the mass of VLDL apoB to yield the FCR of the tracee:

$$FCR = \frac{R_{v0}}{M_v} = \frac{\text{Initial SA Slope}}{\text{Initial SA}}. \qquad \textit{Eq. 6)}$$

This is a very curious result: that for any model (any number of pools and pathways) with equal initial specific activities in all pools, the total production rate (or the fractional catabolic rate) is determined by the initial slope of the specific activity curve. Four important points derive from this observation.

First, for a given set of data, different models that fit the initial decay equally well will yield similar production rates provided each model assumes all VLDL pools to be uniformly labeled initially and to be circulating, intravascular pools. It does not matter how different the models are in the number of pools, connectivity, etc., as long as the initial data are fitted identically. Any difference in estimated production rates can be ascribed to differences in fits of the early part of the curve. It should be noted that if there are noncirculating or extravascular pools, the calculated production rate or FCR will include the flux to such pools.

Second, although not directly relevant to the present discussion, if one could be confident that all pools within VLDL were uniformly labeled, VLDL production could be calculated from studies of extremely short duration, just long enough to characterize the initial slope accurately.

Third, this result is quite different from the commonly used method of calculating FCR from the inverse of the area under the SA curve (scaled by the initial value). The area-under-the-curve formula follows from the occupancy principle (31, 32), which requires that the tracer be introduced into a single compartment which is also the sole point of entry (or the sole point of catabolism) of all of the tracee. Typically, if there is a single intravascular pool (with one or more extravascular pools) and either all synthesis or all catabolism is in the intravascular pool, the occupancy principle holds and the area under the SA curve leads to the correct FCR. Examples would be commonly used models for HDL apoA-I turnover, LDL apoB turnover, and whole body cholesterol turnover. If, however, the tracer labels multiple intravascular pools, the occupancy principle does not hold and the area under the SA curve does not lead to the correct FCR. Thus, the area under the curve after injection of labeled whole VLDL apoB will not yield the correct FCR since VLDL apoB is heterogeneous. On the other hand, the result in equation 6 here is derived from an entirely different set of assumptions, namely, that there are no extravascular pools and that the intravascular pools are all uniformly labeled initially. Models published until now for VLDL apoB turnover satisfy these assumptions so that the initial slopes of the VLDL SA data yield the FCR. The initial slope method is not applicable if there is any extravascular pool, e.g., LDL apoB or HDL apoA-I turnover. Thus, the two results are for two different sets of assumptions that are contradictory (except when the model consists of a single pool). Which result, if either, is correct will depend on the system being studied. Of course, both formulas may be inappropriate in many situations. For instance, the initial slope formula may also be wrong for VLDL apoB due to nonuniform labeling; the area under the curve may also be wrong for LDL apoB or HDL apoA-I due to heterogeneity.

Finally, for the purpose of the present discussion, it will not be necessary for us to solve the model completely when we now consider the effects on the calculated production rate or FCR of assuming homogeneous labeling when in fact the labeling is nonuniform. The initial SA slope will provide the total production rate or FCR that would have been estimated if uniform labeling had been assumed.

If the initial labeling of the pools is not uniform, equation 5 or 6 will not yield the true production rate or the true FCR. Some insight can be gained into the error in these calculations by using equation 2 to substitute for the activity slope in equation 5:

$$R_{v0calc} = \frac{\text{Initial Activity Slope}}{\text{Initial Specific Activity}} = \frac{\sum_{i=1}^{n} R_{0i}u_i}{\sum_{i=1}^{n} m_i u_i}.$$

Therefore

$$\frac{R_{v0calc}}{R_{v0}} = \frac{\sum_{i=1}^{n} \frac{R_{0i}}{R_{v0}} u_i}{\sum_{i=1}^{n} m_i u_i} = \frac{u_e}{u_v}. \qquad \textit{Eq. 7)}$$

Here R_{v0calc} is the production rate calculated under the uniform labeling assumption, which will generally be different from R_{v0}, the true production rate.

We note that the numerator and the denominator are each a weighted mean of the individual specific activities. The denominator, u_v, is the SA of whole VLDL apoB, obtained by weighting the individual SAs by their respective pool mass fractions. Weighting in the numerator is by the fraction of flux out of VLDL from each pool (conversion to IDL and/or LDL as well as direct removal from plasma). If we imagine all the exit fluxes to be combined into a single stream, u_e is the initial specific activity of this stream (immediately after the injection of the tracer bolus). Thus, u_e and u_v are both weighted averages of the specific activities in the different pools, but the weighting is different, by exit fluxes for u_e and by pool masses for u_v.

Thus the ratio, u_e/u_v, which is the ratio of the exit SA to internal or whole VLDL SA, is the factor by which the production rate calculated under the uniform labeling as-

sumption differs from the true production rate. The expression for FCR is the same:

$$\frac{FCR_{calc}}{FCR_{true}} = \frac{\sum_{i=1}^{n} \frac{R_{0i}}{R_{v0}} u_i}{\sum_{i=1}^{n} m_i u_i} = \frac{u_e}{u_v} . \qquad Eq.\ 8)$$

When labeling is actually uniform, the u_i values are all the same. Under this condition, weighting by exit fluxes to get u_e or weighting by mass fractions to get u_v will lead to the same value for u_e and u_v (equal to all the u_i values). Thus, when labeling is uniform, there is no error. When labeling is not uniform, however, these two different weighting methods can lead to very different values for u_e and u_v.

To illustrate these points, we will consider two models: one with multiple inputs and a single output, and the other a two-pool cascade. First consider **Fig. 4,** which shows an n-pool model for VLDL apoB kinetics with arbitrary pathways among the pools and possible de novo secretion into all pools. Outflow (conversion to IDL and/or LDL and direct removal) occurs, however, from just one pool, say pool n. Then u_e equals u_n, and

$$\frac{R_{v0calc}}{R_{v0true}} = \frac{FCR_{calc}}{FCR_{true}} = \frac{u_n}{u_v} . \qquad Eq.\ 9)$$

If the labeling is such that the initial SA in the n-th pool is close to or equal to the SA in whole VLDL, then there is little or no error in assuming uniform labeling to calculate the production rate or FCR. On the other hand, if the initial SA in the n-th pool is very different from the SA in whole VLDL, the R_{v0} or FCR calculated under the uniform labeling assumption can be quite different from the true value. If u_n is twice u_v, the calculated production rate is twice the true rate. If u_n is half of u_v, the calculated production rate is half the true rate. The latter is close to the results in Table 2 for four of five subjects (S_f 60–20 SA vs whole VLDL SA).

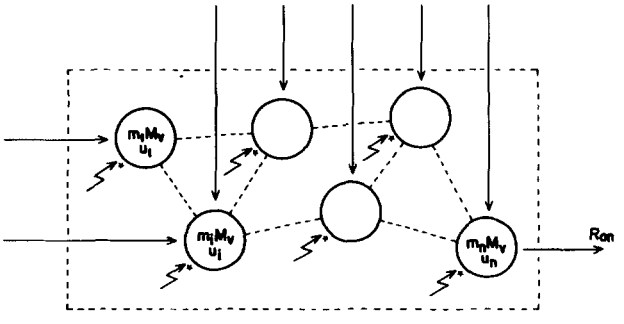

Fig. 4. An n-pool model for the turnover of VLDL apoB, similar to that in Fig. 3, but flux out of VLDL is from only one pool, the n-th pool.

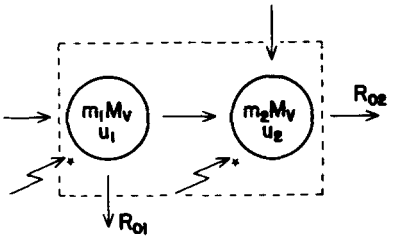

Fig. 5. A two-pool cascade model for the turnover of VLDL apoB. Here, m_1 is the mass fraction in the first pool; m_2 (=1−m_1) is the mass fraction in the second pool; u_1 and u_2 are initial SA in the two pools; R_{01} is the flux out of pool 1, which may be removed from plasma or converted to IDL and/or LDL; R_{02} is the corresponding flux out of pool 2.

A variation on this model, one closer to cascade models used by several investigators to study apoB kinetics in VLDL, would be one with conversion to IDL/LDL (as well as direct removal) from the terminal pool of the cascade (the n-th pool), and slow removal from plasma via a remnant pool, say the r-th pool. Then, the initial exit SA is given by:

$$u_e = \frac{R_{0r}}{R_{v0}} u_r + \frac{R_{0n}}{R_{v0}} u_n .$$

Typically, the flux through the remnant pool is quite small relative to the total flux; that is, R_{0r} is no more than 10% of R_{v0}. It is then reasonable to assume that u_e is quite close to u_n even though there is another exit flux. Hence, equation 9 can still be used to estimate the error in calculating R_{v0} for such a model with an erroneous uniform labeling assumption.

Finally, we will consider a model for VLDL that has no constraints on sites of entry and exit of VLDL. For simplicity of presentation, consider the two-pool cascade shown in **Fig. 5.** Pool 1 represents more buoyant particles, perhaps S_f 400–60, and pool 2 denser particles, perhaps S_f 60–20. Newly secreted VLDL particles may enter either pool while removal from plasma or conversion to IDL/LDL may also take place from either pool. It is easily seen that the initial exit SA is given by

$$u_e = \frac{R_{01}}{R_{v0}} u_1 + \frac{R_{02}}{R_{v0}} u_2 .$$

Initial SA in whole VLDL is given by

$$u_v = m_1u_1 + m_2u_2 .$$

Then, equation 7 becomes

$$\frac{R_{v0calc}}{R_{v0}} = \frac{u_e}{u_v} = \frac{\frac{R_{01}}{R_{v0}} u_1 + \frac{R_{02}}{R_{v0}} u_2}{m_1 u_1 + m_2 u_2}$$

$$= \frac{\frac{R_{01}}{R_{v0}} + \frac{R_{02}}{R_{v0}} \frac{u_2}{u_1}}{m_1 + m_2 \frac{u_2}{u_1}} \qquad \textit{Eq. 10)}$$

We note that $R_{01} + R_{02} = R_{v0}$ and $m_1 + m_2 = 1$. If $u_1 = u_2$, then the numerator and the denominator each equals one, and there is no error. Also, if the exit fluxes are in the same ratio as the masses, i.e., $\frac{R_{02}}{R_{01}} = \frac{m_2}{m_1}$, then $\frac{R_{01}}{R_{v0}} = m_1$ and $\frac{R_{02}}{R_{v0}} = m_2$, so the numerator equals the denominator, and there is no error.

For all other situations, however, the ratio deviates from one. The uniform labeling assumption can lead to overestimation or underestimation. Since the ratio equals $\frac{u_e}{u_v}$, it follows that if u_e exceeds u_v, there is overestimation; if u_v exceeds u_e, there is underestimation. If the pool with higher initial SA contributes more to the exit flux than it does to the total mass, R_{v0} or FCR is overestimated by the uniform labeling assumption; if it contributes less to the exit flux than to the total mass, R_{v0} or FCR is underestimated by the uniform labeling assumption.

These conclusions are portrayed graphically in **Fig. 6**, A-C. Since there are three parameters, $\frac{u_2}{u_1}$, m_2, and $\frac{R_{02}}{R_{v0}}$, that determine the error, a number of curves are shown. For all curves, the abscissa is $\frac{u_2}{u_1}$, the ratio of the specific activities in the two pools, and the ordinate is the ratio of the production rate (or FCR) calculated under the uniform labeling assumption to the true production rate (or FCR).

Each curve shows how the ratio changes as $\frac{u_2}{u_1}$ changes. The different curves in any one panel show the effect of $\frac{R_{02}}{R_{v0}}$, the fraction of total flux that exits from pool 2. The curves numbered 1-6 correspond to six different values of $\frac{R_{02}}{R_{v0}}$, 0.1, 0.3, 0.5, 0.7, 0.9, and 1.0, respectively. Each panel is for a different value of m_2 (the fraction of total mass in pool 2).

It may be noted that all curves meet at $\frac{u_2}{u_1} = 1$ since there is no error if labeling is uniform. Also, for each value of m_2, if $\frac{R_{02}}{R_{v0}}$ equals m_2, the curve is horizontal at 1,

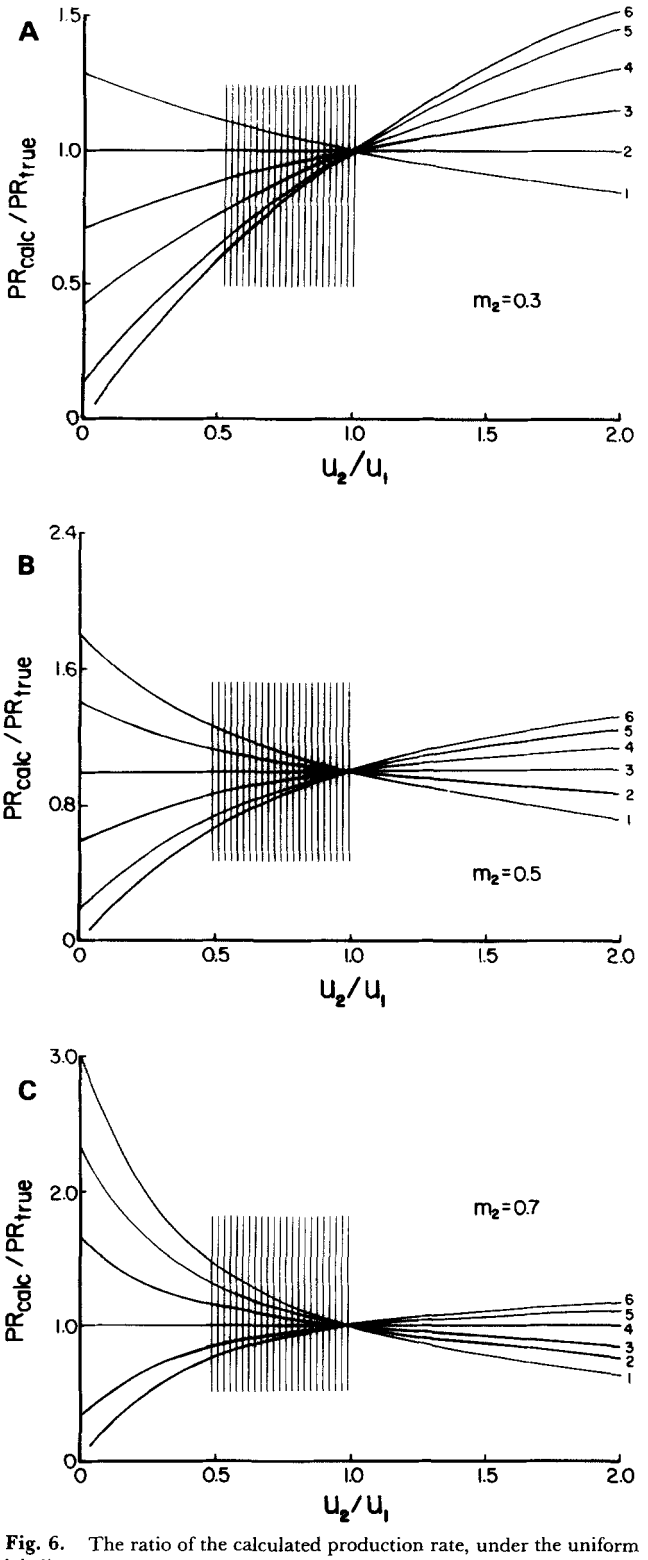

Fig. 6. The ratio of the calculated production rate, under the uniform labeling assumption, to the true production rate, as a function of the ratio of specific activities in the two pools of the model shown in Fig. 5; A, the case with 30% of the total mass in pool 2; B, 50%; C, 70%. In each panel, the curves numbered 1-6 correspond to six different values of $\frac{R_{02}}{R_{v0}}$ (the fraction of total flux that exits from pool 2) – 0.1, 0.3, 0.5, 0.7, 0.9, and 1.0, respectively. The highlighted regions correspond to the range of specific activity ratios that we have observed.

meaning no error even if labeling is not uniform (curve 2 in Fig. 6A, 3 in Fig. 6B, and 4 in Fig. 6C).

As $\frac{u_2}{u_1}$ increases, overestimates decline until they become underestimates, and underestimates move closer to one until they become overestimates.

The effect of increasing $\frac{R_{02}}{R_{v0}}$, the exit fraction from pool 2, depends on whether u_2 is larger or smaller than u_1. If u_2 is smaller than u_1, increasing $\frac{R_{02}}{R_{v0}}$ decreases u_e and consequently the estimated production rate. (An overestimate becomes more correct and then an underestimate; an underestimate becomes more of an underestimate.) On the other hand, if u_2 is larger than u_1, increasing $\frac{R_{02}}{R_{v0}}$ increases u_e and consequently the estimated production rate. (An underestimate becomes more correct and then an overestimate; an overestimate becomes more of an overestimate.) This can be seen by looking at different curves in a single panel at a particular value of the abscissa, $\frac{u_2}{u_1}$.

The effect of m_2 is generally the opposite of that of $\frac{R_{02}}{R_{v0}}$. If u_2 is smaller than u_1, increasing m_2 decreases u_v in relation to u_e and consequently increases the estimated production rate. If u_2 exceeds u_1, increasing m_2 increases u_v in relation to u_e and consequently decreases the estimated production rate. This can be seen by looking at the three curves for any single $\frac{R_{02}}{R_{v0}}$ (one given in each panel) at a particular value of the abscissa, $\frac{u_2}{u_1}$.

Finally, we have attempted, by highlighting the regions of the curves generated by values for $\frac{u_2}{u_1}$ in the range we have observed, to provide the reader with an estimate of the magnitude of the error for various values of $\frac{R_{02}}{R_{v0}}$ and m_2. In general, overestimates of 50% and underestimates of 30% for the production rate or FCR are possible.

In summary, we have consistently observed nonhomogeneous labeling of VLDL subfractions isolated by both physical and immunochemical methods. We have attempted to define the effects of nonhomogeneous labeling on the mathematical analysis of SA data in order to provide investigators with a sense of the significance of erroneously assuming homogeneous labeling. We realize that the heterogeneity is likely to be more complex than we show in this study, that is, more subfractionation will demonstrate further nonhomogeneity, and that there is a limit to practical approaches to this problem. In particular, when we analyze apoB SA data from individual S_f subfractions, it is quite likely that each subfraction will require more than one pool. In that case, the initial labeling of the multiple pools within any subfraction will have to be addressed. We believe, however, that identification of nonhomogeneous labeling, and inclusion of such data in the modeling process, may provide new insights into the kinetics of apolipoprotein transport.

This work was supported by the following grants from the NIH-NHLBI: HL-36000, HL-21006, and RR-645.

Manuscript received 13 July 1988; in revised form 13 June 1989; in re-revised form 24 October 1989; accepted 12 February 1990.

REFERENCES

1. Langer, T., W. Strober, and R. I. Levy. 1972. The metabolism of low density lipoprotein in familial type II hyperlipoproteinemia. *J. Clin. Invest.* **51:** 1528–1536.
2. Janus, E. D., A. Nicoll, R. Wootton, P. R. Turner, P. J. Magill, and B. Lewis. 1980. Quantitative studies of very low density lipoprotein: conversion to low density lipoprotein in normal controls and primary hyperlipidaemic states and the role of direct secretion of low density lipoprotein in heterozygous familial hypercholesterolaemia. *Eur. J. Clin. Invest.* **10:** 149–159.
3. Bilheimer, D. W., N. J. Stone, and S. M. Grundy. 1979. Metabolism studies in familial hypercholesterolemia: evidence for a gene-dose effect in vivo. *J. Clin. Invest.* **64:** 524–533.
4. Fisher, W. R., L. A. Zech, P. Bardalaye, G. Warmke, and M. Berman. 1980. The metabolism of apolipoprotein B in subjects with hypertriglyceridemia and polydisperse LDL. *J. Lipid Res.* **21:** 760–774.
5. Chait, A., J. J. Albers, and J. D. Brunzell. 1980. Very low density lipoprotein overproduction in genetic forms of hypertriglyceridemia. *Eur. J. Clin. Invest.* **10:** 17–22.
6. Reardon, M. F., N. H. Fidge, and P. J. Nestel. 1978. Catabolism of very low density lipoprotein B apoprotein in man. *J. Clin. Invest.* **61:** 850–860.
7. Kissebah, A. H., S. Alfarsi, and P. W. Adams. 1981. Integrated regulation of very low density lipoprotein triglyceride and apolipoprotein-B kinetics in man: normolipemic subjects, familial hypertriglyceridemia and familial combined hyperlipidemia. *Metabolism.* **30:** 856–868.
8. Packard, C. J., J. Shepherd, S. Joerns, A. M. Gotto, and O. D. Taunton. 1980. Apolipoprotein B metabolism in normal, type IV and type V hyperlipoproteinemic subjects. *Metabolism.* **29:** 213–222.
9. Janus, E. D., A. M. Nicoll, P. R. Turner, P. Magill, and B. Lewis. 1980. Kinetic bases of the primary hyperlipidaemias: studies of apolipoprotein B turnover in genetically defined subjects. *Eur. J. Clin. Invest.* **10:** 161–172.
10. Turner, P. R., C. Cortese, R. Wootton, C. Marenah, N. E. Miller, and B. Lewis. 1985. Plasma apolipoprotein B metabolism in type III dysbetalipoproteinemia. *Eur. J. Clin. Invest.* **15:** 100–112.
11. Gregg, R. E., and H. B. Brewer. 1986. The role of apolipoprotein E in modulating the metabolism of apolipoprotein B-48- and apolipoprotein B-100-containing lipoproteins in humans. *Adv. Exp. Med. Biol.* **201:** 289–298.
12. Schaefer, E. J., R. E. Gregg, G. Ghiselli, T. M. Forte, J. M. Ordovas, L. A. Zech, and H. B. Brewer. 1986. Familial apolipoprotein E deficiency. *J. Clin. Invest.* **78:** 1206–1219.

13. Ginsberg, H. N., N. A. Le, I. J. Goldberg, J. C. Gibson, A. Rubinstein, P. W. Iverson, R. Norum, and W. V. Brown. 1986. Apolipoprotein B metabolism in subjects with deficiency of apolipoproteins C-III and A-I. *J. Clin. Invest.* **78:** 1287–1295.
14. Bilheimer, D. W., S. Eisenberg, and R. I. Levy. 1972. The metabolism of very low density lipoprotein proteins. I. Preliminary in vitro and in vivo observations. *Biochim. Biophys. Acta.* **260:** 212–221.
15. Eisenberg, S., and D. Rachmilewitz. 1973. Metabolism of rat plasma very low density lipoprotein. I. Fate in circulation of the whole lipoprotein. *Biochim. Biophys. Acta.* **326:** 378–390.
16. Berman, M. 1982. Kinetic analysis and modeling: theory and applications to lipoproteins. *In* Lipoprotein Kinetics and Modeling. M. Berman, S. M. Grundy, and B. V. Howard, editors. Academic Press, New York. 4–36.
17. Melish, J., N. A. Le, H. N. Ginsberg, D. Steinberg, and W. V. Brown. 1980. Dissociation of apoprotein B and triglyceride production in very-low-density lipoprotein. *Am. J. Physiol.* **239:** E354–E362.
18. Ginsberg, H. N., N. A. Le, J. Melish, D. Steinberg, and W. V. Brown. 1981. Effect of a high carbohydrate diet on apoprotein-B catabolism in man. *Metabolism.* **30:** 347–353.
19. Berman, M., M. Hall III, R. I. Levy, S. Eisenberg, D. W. Bilheimer, R. D. Phair, and R. H. Goebel. 1978. Metabolism of apoB and apoC lipoproteins in man: kinetic studies in normal and hyperlipoproteinemic subjects. *J. Lipid Res.* **19:** 38–55.
20. Eaton, R. P., R. C. Allen, and D. S. Schade. 1983. Overproduction of a kinetic subclass of VLDL-apoB, and direct catabolism of VLDL-apoB in human endogenous hypertriglyceridemia: an analytical model solution of tracer data. *J. Lipid Res.* **24:** 1291–1303.
21. Ginsberg, H. N., N. A. Le, and J. C. Gibson. 1985. Regulation of the production and catabolism of plasma low density lipoprotein in hypertriglyceridemia. *J. Clin. Invest.* **75:** 614–623.
22. Beltz, W. F., Y. A. Kesaniemi, B. V. Howard, and S. M. Grundy. 1985. Development of an integrated model for analysis of the kinetics of apolipoprotein B in plasma very low density lipoproteins, intermediate density lipoproteins, and low density lipoproteins. *J. Clin. Invest.* **76:** 575–585.
23. Packard, C. J., A. Munro, A. R. Lorimer, A. M. Gotto, and J. Shepherd. 1984. Metabolism of apolipoprotein B in large triglyceride-rich very low density lipoproteins of normal and hypertriglyceridemic subjects. *J. Clin. Invest.* **74:** 2178–2192.
24. McFarlane, A. S. 1958. Efficient trace-labeling of proteins with iodine. *Nature (London).* **182:** 53–57.
25. Lindgren, F. T., L. C. Jensen, and F. T. Hatch. 1972. *In* Blood Lipids and Lipoproteins: Quantitation, Composition and Metabolism. G. J. Nelson, editor. John Wiley and Sons, New York. 181–274.
26. Ginsberg, H. N., N. Ngai, and J. Lee. 1987. Immunoaffinity isolation and initial characterization of apolipoprotein E-rich and E-deficient subclasses of very low density lipoproteins. *Arteriosclerosis.* **7:** 503 (Abstract).
27. Le, N. A., J. S. Melish, B. C. Roach, H. N. Ginsberg, and W. V. Brown. 1978. Direct measurement of apoprotein B specific activity in ^{125}I-labeled lipoproteins. *J. Lipid Res.* **19:** 578–584.
28. Egusa, G., D. W. Brady, S. M. Grundy, and B. V. Howard. 1983. Isopropanol precipitation method for the determination of apolipoprotein B specific activity and plasma concentrations during metabolic studies of very low density lipoprotein and low density lipoprotein apolipoprotein B. *J. Lipid Res.* **24:** 1261–1267.
29. Ishikawa, Y., C. J. Fielding, and P. E. Fielding. 1988. A change in apolipoprotein B expression is required for the binding of apolipoprotein E to very low density lipoprotein. *J. Biol. Chem.* **263:** 2744–2749.
30. Krul, E. S., M. J. Tikkanen, T. G. Cole, J. M. Davie, and G. Schonfeld. 1985. Role of apolipoproteins B and E in the cellular binding of very low density lipoproteins. *J. Clin. Invest.* **75:** 361–369.
31. Orr, J. S., and F. C. Gillespie. 1968. Occupancy principle for radioactive tracers in steady-state biological systems. *Science.* **162:** 138–139.
32. Ramakrishnan, R., E. F. Leonard, and R. B. Dell. 1984. A proof of the occupancy principle and the mean-transit-time theorem for compartmental models. *Math. Biosci.* **68:** 121–136.